Mon. Not. R. Astron. Soc. **357,** 471–477 (2005) doi:10.1111/j.1365-2966.2005.08611.x

Calculated spectra for HeH^+ and its effect on the opacity of cool metal-poor stars

Elodie A. Engel, Natasha Doss, Gregory J. Harris and Jonathan Tennyson★
Department of Physics and Astronomy, University College London, London WC1E 6BT

Accepted 2004 November 4. Received 2004 November 4; in original form 2004 July 28

ABSTRACT

The wavelength and Einstein *A* coefficient are calculated for all rotation–vibration transitions of $^4He^1H^+$, $^3He^1H^+$, $^4He^2H^+$ and $^3He^2H^+$, giving a complete line list and the partition function for $^4HeH^+$ and its isotopologues. This opacity is included in the calculation of the total opacity of low-metallicity stars and its effect is analysed for different conditions of temperature, density and hydrogen number fraction. For a low helium number fraction (as in the Sun), it is found that HeH^+ has a visible but small effect for very low densities ($\rho \leqslant 10^{-10}$ g cm^{-3}), at temperatures around 3500 K. However, for high helium number fraction, the effect of HeH^+ becomes important for higher densities ($\rho \leqslant 10^{-6}$ g cm^{-3}), its effect being most important for a temperature around 3500 K. Synthetic spectra for a variety of different conditions are presented.

Key words: molecular data – plasmas – infrared: general.

1 INTRODUCTION

HeH^+ is thought to be the first molecular species to appear in the Universe (Lepp, Stancil & Dalgarno 2002). Consequently, stars formed from primordial material should contain some HeH^+. Such stars probably exist, and Kashlinsky & Rees (1983) proposed a route by which stars of mass as low as 0.2 $M_\odot$ could be formed from primordial material. Moreover, the recent discovery of the very metal-poor star HE 0107–5240 (Christlieb et al. 2002) has added credence to the possibility that low-mass primordial stars were formed. Observing such stars would provide much information about the early Universe, and could give an estimate of its age. Then, HeH^+ could influence their formation and evolution. To have accurate information about the stellar formation and evolution, we need to have the necessary opacity data.

For zero-metallicity stars, the only contributors to the opacity are the various hydrogen and helium species, ions and electrons. Many hydrogen and helium species have already been included in calculated opacity of zero-metallicity stars but HeH^+ has always been neglected in such calculations (Harris et al. 2004a). However, HeH^+ could be important because of its strong electric dipole moment. There appears to be no available opacity data for HeH^+ and its isotopologues. Such an opacity is calculated in this work. These calculations provide predictions of the line intensity of HeH^+, which also could be used to search for this molecular ion in the Universe.

There have been several previous attempts to detect extraterrestrial HeH^+, none conclusive. Moorhead et al. (1988) tried to detect HeH^+ in the planetary nebula NGC 7027 but failed. According to Cecchi-Pestellini & Dalgarno (1993), this failure arose from an incorrect estimate of the chemistry of HeH^+ and hence of its concentration in the planetary nebula. Furthermore Moorhead et al. (1987) may not have observed the right volume of the nebula. Miller et al. (1992) tentatively identified two emission features in the spectra of Supernova 1987A as due to HeH^+. This observation has not been confirmed. The HeH^+ $j = 1-0$ rotational emission line may have been observed by the Infrared Space Observatory in NGC 7027 (Liu et al. 1997). Its identification is complicated by the near coincidence of its 149.14-μm rotational transition with the 149.09- and 149.39-μm lines of CH. Moreover, Rabadan, Sarpal & Tennyson (1998) found that the electron impact excitation rate to the $j = 2$ rotational level from $j = 0$ is half that for $j = 1-0$. As a result, observation of both $j = 2-1$ and $j = 1-0$ emission lines should be possible. Observation of both these would give a much more secure detection of HeH^+.

Having accurate theoretical predictions for the spectrum of low-metallicity stars should help to determine the best conditions to search for and detect HeH^+. Knowing the spectrum of HeH^+ should also aid its detection in other astrophysical environments. Zygelman, Stancil & Dalgarno (1998) investigated the possibility for enhancement of the rate of formation of HeH^+ in astrophysical environments when stimulated by the cosmic background radiation field. They found that the effects on the fractional abundance of HeH^+ are small in the early Universe, in supernova ejecta and in planetary nebulae but may be important in quasar broad-line clouds.

As our calculations show (see below), it could be possible to detect HeH^+ in cool helium stars. Such stars exist, and Saio & Jeffery (2000) have observed and studied helium stars, and particularly V625 Her, for more than 20 years. They showed that the merger of two white dwarfs could lead to an extreme helium star (containing a

★E-mail: j.tennyson.ucl.ac.uk

number fraction of helium around 0.9). On the other hand, Bergeron & Leggett (2002) studied two cool white dwarfs, SDSS 1337+00 and LHS 3250, and found that their observed energy distributions were best reproduced by models of cool extreme helium stars, and so these stars should be such objects. However, they did not take account of HeH^+ in their atmosphere models (Bergeron, Leggett & Ruiz 2001). Similarly Stancil (1994) investigated the effect of the opacities of He_2^+ and H_2^+ in cool white dwarfs but neglected the effect of HeH^+ which is, however, a more stable ion.

In this work we will investigate the effect of HeH^+ on the opacity of zero-metallicity stars. In Section 2 we will describe the steps leading to the calculation of the energy levels of all stable isotopologues of HeH^+ and compute a spectroscopic line list and their partition function. In Section 3 we explain how the opacity functions were calculated and use them in models of metal-poor stars for different temperatures, densities and hydrogen number fractions. Finally, results are discussed in Section 4.

2 CALCULATION OF THE LINE LIST

2.1 Transition data

The program LEVEL 7.5 (Le Roy 2002) was used to obtain rotation–vibration transition frequencies and Einstein *A* coefficients. The core of the program determines discrete eigenvalues and eigenfunctions of the radial Schrödinger equation. We used LEVEL to calculate the number, energy and wavefunction of each rotation–vibration level for a given one-dimensional potential. These were then used to calculate Einstein *A* coefficients for dipole transitions between all bound rotation–vibration levels of each isotopologue.

The Schrödinger equation which is numerically solved by the program is

$$-\frac{\hbar^2}{2\mu}\frac{d^2\psi_{v,J}(R)}{\mathrm{d}R^2} + V_J(R)\psi_{v,J}(R) = E_{v,J}\psi_{v,J}(R) \tag{1}$$

where μ is the effective reduced mass of the system, J the rotational quantum number, v the vibrational quantum number, and $V_J(R)$ is the effective potential of the molecule, R being the distance between the two atoms of the molecule. $V_J(R)$ is defined by

$$V_J(R) = V_{\mathrm{BO}}(R) + \frac{J(J+1)}{2\mu R^2} + \frac{V_{\mathrm{ad}}(R)}{\mu} \tag{2}$$

where V_{BO} is the potential in the Born–Oppenheimer approximation and V_{ad} are the adiabatic corrections.

The core of the calculation is to determine the eigenvalues $E_{v,J}$ and eigenfunctions $\psi_{v,J}(R)$ of the effective potential $V_J(R)$. In order to obtain such information, one has to provide input data to the program. The physical data are the masses of the atoms of the diatomic molecule, its effective potential as a function of the internuclear distance R and the dipole moment, also as a function of the internuclear distance R.

For each isotopologue, V_{BO} was that calculated using the Born–Oppenheimer approximation by Kolos & Peek (1976). This potential was corrected for adiabatic effects (Bishop & Cheung 1979), which accounts for some of the coupling between electronic and nuclear motion. The corrections were given by Bishop & Cheung (1979) for $^4HeH^+$ but as $^4HeH^+$ and its isotopologues $^4HeD^+$, $^3HeH^+$ and $^3HeD^+$ only differ in their reduced mass, we just had to replace the $^4HeH^+$ reduced mass by the reduced mass of the appropriate isotopologue.

The effective potential allows for adiabatic effects. Adjusting the masses allows, at least partially, for non-adiabatic effects. We calculated energy levels for several reduced masses given by Coxon & Hajigeorgiou (1999). We tested the nuclear reduced mass, μ_{nucl}, which does not take account of the electrons, the atomic reduced mass μ_{at}, which takes full account of the electrons and the effective, μ_{eff}, and dissociation, μ_{diss}, reduced masses which have intermediate values. We compared our transition frequencies calculated using the dipole selection rules ($\Delta J = \pm 1$, Δv any) with the experimental transition frequencies tabulated by Coxon & Hajigeorgiou (1999). The results are summarized in Tables 1 and 2. Use of the dissociation reduced mass leads to the best results (see Tables 1 and 2). Since the dissociation reduced mass is the most appropriate for high-lying (near dissociation) levels, it should also be the best for levels yet to be observed experimentally. We therefore used this mass for all further calculations presented here.

Using SI units, the Einstein $A_{(v'J')\to(v''J'')}$ coefficient is related to the transition dipole by

$$|\langle\psi_{v'J'}|\mu|\psi_{v''J''}\rangle|^2 = \frac{2J'+1}{(2J''+1)\nu^3}A_{(v'J')\to(v''J'')}. \tag{3}$$

Table 1. Difference between the experimental rotation–vibration transition frequencies and the theoretical ones calculated with different reduced masses for $^4HeH^+$; the experimental frequencies and the reduced masses are from Coxon & Hajigeorgiou (1999).

			Experiment (cm^{-1})	Difference obs − calc (cm^{-1})			
v'	v''	J	P(J) transition	μ_{nucl}	μ_{at}	μ_{eff}	μ_{diss}
1	0	1	2843.9035	0.284	−0.457	−0.036	0.216
		2	2771.8059	0.279	−0.418	−0.022	0.215
		3	2695.0500	0.278	−0.371	−0.002	0.218
		4	2614.0295	0.278	−0.320	0.020	0.223
		5	2529.134	0.278	−0.266	0.043	0.228
		6	2440.742	0.276	−0.211	0.066	0.231
		9	2158.140	0.268	−0.037	0.136	0.240
		10	2059.210	0.260	0.019	0.156	0.238
		11	1958.388	0.250	0.074	0.174	0.234
		12	1855.905	0.243	0.132	0.195	0.233
		13	1751.971	0.225	0.181	0.206	0.221
2	1	1	2542.531	0.069	−0.492	−0.173	0.018
		2	2475.814	0.067	−0.456	−0.159	0.019
		5	2248.854	0.064	−0.319	−0.102	0.029
		6	2165.485	0.070	−0.260	−0.072	0.040
		7	2078.841	0.091	−0.184	−0.027	0.066
		8	1989.251	0.089	−0.129	−0.005	0.069
		9	1896.992	0.106	−0.053	0.038	0.092
		10	1802.349	0.114	0.016	0.072	0.105
		11	1705.543	0.121	0.085	0.105	0.117
		19	862.529	0.106	0.651	0.341	0.156
		20	745.624	0.099	0.744	0.377	0.158
3	2	5	1966.356	0.043	−0.175	−0.051	0.023
		17	833.640	0.096	0.650	0.336	0.147
		18	719.769	0.098	0.752	0.380	0.158
5	4	11	901.963	0.060	0.522	0.259	0.102
		12	807.806	0.078	0.614	0.309	0.127
6	5	8	863.378	0.048	0.521	0.252	0.092
		9	782.925	0.044	0.575	0.274	0.093
7	6	4	817.337	0.127	0.624	0.342	0.173
		5	760.367	0.151	0.681	0.380	0.200
7	5	12	938.200	−0.327	1.758	0.573	−0.136

Table 2. Difference between the experimental pure rotational transition frequencies and the theoretical ones calculated with different reduced masses for ^{4}HeH$^+$; the experimental results and the reduced masses are from Coxon & Hajigeorgiou (1999).

			Experiment (cm^{-1})		Difference obs − calc (cm^{-1})		
v	J''	J'	frequency	μ_{nucl}	μ_{at}	μ_{eff}	μ_{diss}
0	0	1	67.053	0.002	−0.037	−0.015	−0.002
	1	2	133.717	0.004	−0.074	−0.030	−0.003
	6	7	448.160	0.007	−0.244	−0.102	−0.016
	10	11	657.221	0.026	−0.313	−0.121	−0.005
	11	12	701.317	0.020	−0.333	−0.132	−0.012
	12	13	741.706	0.026	−0.336	−0.130	−0.007
	13	14	778.224	0.032	−0.335	−0.127	−0.002
	14	15	810.708	0.038	−0.330	−0.121	0.004
	15	16	839.010	0.042	−0.322	−0.115	0.009
	16	17	862.984	0.043	−0.313	−0.110	0.011
	17	18	882.475	0.047	−0.297	−0.102	0.015
	18	19	897.334	0.035	−0.290	−0.106	0.005
	20	21	912.242	0.036	−0.234	−0.080	0.011
	21	22	911.704	0.033	−0.200	−0.068	0.011
	23	24	891.888	0.035	−0.087	−0.018	0.024
	24	25	870.298	0.028	−0.009	0.012	0.025
	25	26	837.180	0.033	0.133	0.076	0.042
1	10	11	598.829	0.018	−0.270	−0.107	−0.009
	11	12	637.767	0.013	−0.282	−0.114	−0.014
	12	13	672.989	0.009	−0.291	−0.120	−0.019
	13	14	704.270	0.019	−0.281	−0.111	−0.009
	14	15	731.430	0.016	−0.280	−0.112	−0.012
	15	16	754.235	0.019	−0.266	−0.104	−0.007
	16	17	772.464	0.017	−0.253	−0.100	−0.008
	17	18	785.837	0.015	−0.235	−0.093	−0.008
	18	19	793.997	0.023	−0.197	−0.072	0.003
	19	20	796.490	0.027	−0.156	−0.052	0.010
	20	21	792.616	0.032	−0.101	−0.025	0.020
	21	22	781.245	0.048	−0.019	0.019	0.042
	22	23	760.340	0.030	0.061	0.043	0.033
	23	24	724.933	0.043	0.254	0.135	0.063
2	13	14	627.320	0.019	−0.207	−0.079	−0.002
	14	15	648.324	0.014	−0.200	−0.078	−0.005
	15	16	664.559	0.015	−0.180	−0.069	−0.003
	16	17	675.609	0.012	−0.156	−0.061	−0.003
	17	18	680.895	0.014	−0.119	−0.044	0.001
	18	19	679.586	0.019	−0.064	−0.017	0.011
	19	20	670.340	0.024	0.010	0.018	0.023
	20	21	650.613	0.025	0.118	0.065	0.033

We used the electric dipole moment data for ^{4}HeH$^+$ given in Saenz (2003). These data could not be used directly as Saenz tabulates only the electronic dipole moment which is the contribution of the electrons to the dipole moment, without taking account of the nuclear charges of H and He. To use these data we first had to take account of H and He and then to translate the dipole to the centre of mass for each isotopologue, our results are given in Table 3.

Thus we obtained a line list of ^{4}HeH$^+$, ^{3}HeH$^+$, ^{4}HeD$^+$ and ^{3}HeD$^+$ transitions. Table 4 gives part of the line list: the astronomically most important transitions for ^{4}HeH$^+$. The full line list for this main isotopologue which contains 1431 lines, and the minor variants, are available in electronic form at http://www.blackwellpublishing.com/products/journals/suppmat/MNR/MNR8611/MNR8611sm.htm and at the Centre de Données astronomiques de Strasbourg (CDS).[1] These tables use the standard Kurucz format (Kurucz 2000).

Table 3. Dipole moment, in atomic units, as a function of internuclear separation, R, for the electronic ground state of ^{4}HeH$^+$ and isotopologues. The electronic contribution is taken from Saenz (2003).

R/a_0	^{4}HeH$^+$	^{3}HeH$^+$	^{4}HeD$^+$	^{3}HeD$^+$
0.6	0.14879	0.11879	0.06879	0.02879
0.8	0.24025	0.20025	0.13358	0.08025
1.0	0.35267	0.30267	0.21934	0.15267
1.1	0.41620	0.36120	0.26953	0.19620
1.2	0.48426	0.42426	0.32426	0.24426
1.3	0.55658	0.49158	0.38325	0.29658
1.4	0.63288	0.56288	0.44621	0.35288
1.45	0.67245	0.59995	0.47912	0.38245
1.5	0.71291	0.63791	0.51291	0.41291
1.6	0.79641	0.71641	0.58308	0.47641
1.8	0.97277	0.88277	0.73277	0.61277
2.0	1.15986	1.05986	0.89319	0.75986
2.2	1.35549	1.24549	1.06216	0.91549
2.4	1.55743	1.43743	1.23743	1.07743

2.2 The partition function

The internal partition function is defined by

$$Q_{vr} = \sum_i g_i \exp\left(\frac{-E_i}{kT}\right) \tag{4}$$

where k is Boltzmann's constant. The energy of the ith level relative to the vibration–rotation ground state is given by E_i and its degeneracy by g_i. g_i is given by $(2J + 1)$. As we computed all the energy levels, we used this data list and made a direct summation of each level i. The partition functions of ^{4}HeH$^+$ and its isotopologues are given in Table 5.

We fitted the partition functions of the isotopologues to the standard form of Irwin (1981):

$$\log Q_{vr} = \sum_{n=0}^{n=5} a_n [\log(\theta)]^n \tag{5}$$

where $\theta = 5040/T$. The coefficients a_n are given in Table 6.

This fit reproduces our partition function data between 500 and 10 000 K, to a standard deviation on $\log Q_{vr}$ better than 1.5×10^{-3}. For ^{4}HeH$^+$, our results agree reasonably with those of Sauval and Tatum, although our Q_{vr} is significantly lower at high temperatures. We know of no data on the partition function for the other isotopologues.

3 THE OPACITY OF ZERO-METALLICITY STARS

3.1 The opacity of HeH$^+$

The monochromatic opacity or absorption coefficient κ_ν is given by the relation

$$\kappa_\nu = \sum_i S_i f_i(\nu - \nu_{i0}) \tag{6}$$

[1] http://cdsweb.u-strasbg.fr/

Table 4. A sample of the $^4HeH^+$ line list, covering some of the lines most important to astronomy. We present tha data in the format used by Kurucz (1993). The complete list can be obtained in electronic form at http://www.blackwellpublishing.com/products/journals/suppmat/MNR/MNR8611/MNR8611sm.htm and via CDS (http://cdsweb.u-strasbg.fr/).

λ (nm)	A (s^{-1})	J'	E' (cm^{-1})	J''	E'' (cm^{-1})	code v' label′	v'' label″	iso
1770.0593	0.428986E+02	3.0	5850.293	2.0	200.765	102X 2	X 0	14
1780.5247	0.384090E+02	2.0	5683.373	1.0	67.051	102X 2	X 0	14
1794.8580	0.305583E+02	1.0	5571.471	0.0	0.000	102X 2	X 0	14
1835.4404	0.824290E+02	0.0	5515.334	1.0	67.051	102X 2	X 0	14
1861.9524	0.517642E+02	1.0	5571.471	2.0	200.765	102X 2	X 0	14
3248.6434	0.365347E+03	3.0	3278.973	2.0	200.765	102X 1	X 0	14
3301.8692	0.341654E+03	2.0	3095.638	1.0	67.051	102X 1	X 0	14
3363.8480	0.283663E+03	1.0	2972.786	0.0	0.000	102X 1	X 0	14
3516.0271	0.830802E+03	0.0	2911.170	1.0	67.051	102X 1	X 0	14
3607.4759	0.542764E+03	1.0	2972.786	2.0	200.765	102X 1	X 0	14
50098.8713	0.375132E+01	3.0	400.370	2.0	200.765	102X 0	X 0	14
74786.5782	0.104399E+01	2.0	200.765	1.0	67.051	102X 0	X 0	14
149140.4805	0.109163E+00	1.0	67.051	0.0	0.000	102X 0	X 0	14

Table 5. Partition functions of $^4HeH^+$, $^3HeH^+$, $^4HeD^+$ and $^3HeD^+$ calculated by direct summation and by Sauval & Tatum (1984).

T [K]	$^4HeH^+$	$^4HeH^{+a}$	$^3HeH^+$	$^4HeD^+$	$^3HeD^+$
10	1.00		1.00	1.01	1.00
20	1.02		1.02	1.16	1.12
50	1.45		1.40	2.09	1.93
100	2.44		2.32	3.78	3.45
200	4.51		4.26	7.20	6.54
400	8.69		8.19	14.11	12.77
600	12.93		12.17	21.17	19.12
800	17.28		16.24	28.59	25.76
1000	21.84	20.36	20.51	36.62	32.90
1500	34.79	32.36	32.53	60.43	53.87
2000	50.76	47.66	48.28	90.91	80.53
2500	70.54	66.55	65.52	129.45	114.10
3000	94.80	89.33	87.83	177.32	155.70
3500	123.90	116.35	114.58	235.36	206.00
4000	157.84	147.93	145.77	303.68	265.09
4500	196.32	184.42	181.10	381.76	332.47
5000	238.77	226.19	220.08	468.57	407.23
5500	284.56	273.61	262.10	562.82	488.24
6000	333.00	327.04	306.55	663.12	574.31
6500	383.44	386.87	352.82	768.13	664.27
7000	435.30	453.51	400.38	876.59	757.06
7500	488.05	527.35	448.75	987.41	851.74
8000	541.27	608.81	497.54	1099.61	947.50
8500	594.57	698.32	546.40	1212.41	1043.66
9000	647.67	796.29	595.07	1325.12	1139.65

Note: [a]Sauval & Tatum (1984).

where for the particular combination of units of dipole moment in Debye, Einstein A coefficients in s^{-1} and wavenumber in cm^{-1}, the integrated intensity S_i, in cm per molecule, is given by

$$S_i = \frac{1.3271 \times 10^{-12}(2J'+1)}{Q_{\rm vr}\nu^2} \exp\left(\frac{-E''}{kT}\right) \times \left[1 - \exp\left(\frac{-hc\nu}{kT}\right)\right] A_{(v'J')\rightarrow(v''J'')}. \quad (7)$$

f_i is the line profile, which is assumed to result from the Doppler effect, ν_{i0} is the central frequency of line i and ν is the frequency where the monochromatic opacity is calculated. To calculate κ_ν we took account of the lines whose frequency ν_{i0} was in the region $[\nu - \Delta\nu, \nu + \Delta\nu]$. The opacity function for one species is the set of all the values $\kappa_\nu(\nu)$. So to compute the opacity function of the molecular ion HeH^+, we had to obtain κ_ν for all frequencies. We calculated the opacity functions of all the isotopologues of HeH^+ and included them in the program LoMES (Harris et al., in preparation) to take account of them in the calculation of the total opacity; see next section. In Fig. 1 we give the opacity of $^4HeH^+$. Inspecting this shows that we can already assume that this molecular ion will only have an effect on the opacity for wavenumbers under 5000 cm^{-1}.

3.2 Calculation of the total opacity

We used program LoMES, which was written to calculate the effect of H_3^+ (Harris et al. 2004a). This program calculates the frequency-dependent continuous opacity, which is the total opacity. It uses the subroutines developed by Booth and Lynas-Grey

Table 6. Coefficients a_n for the partition function of ^{4} HeH^+, ^{3} HeH^+, ^{4} HeD^+ and ^{3} HeD^+.

a_n	$^4HeH^{+a}$	$^4HeH^+$	$^3HeH^+$	$^4HeD^+$	$^3HeD^+$
a_0	2.3613E+00	2.3825221100E+00	2.3470739949E+00	2.6757191008E+00	2.6146821959E+00
a_1	−1.9733E+00	−1.8465826509E+00	−1.8389007330E+00	−1.9297696419E+00	−1.9106499446E+00
a_2	6.7610E−01	−5.7262657474E−02	−4.4833084371E−02	−1.1379258988E−01	−1.0812923547E−01
a_3	7.9400E−02	1.6336545830E+00	1.6365741096E+00	1.6385861847E+00	1.6373479252E+00
a_4		−1.3736584708E+00	−1.4037963642E+00	−1.2822076706E+00	−1.2855341298E+00
a_5		2.9469135285E−01	3.1100448067E−01	2.5768531906E−01	2.5467446472E−01

Note: [a]Sauval & Tatum (1984).

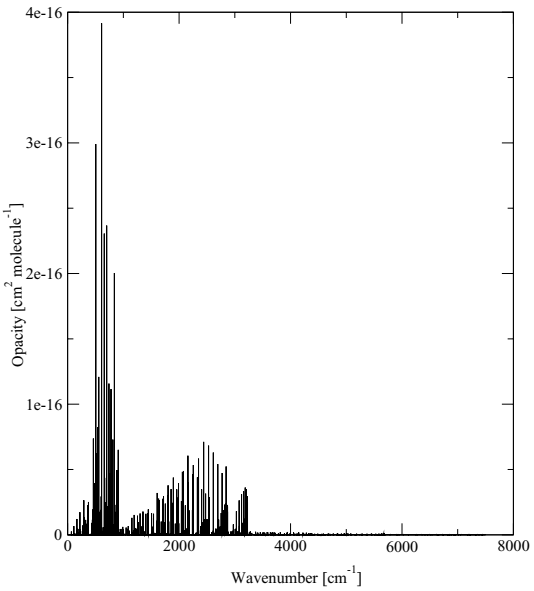

Figure 1. Opacity of ^{4}HeH$^+$ at a temperature $T = 3500$ K.

(2002, private communication) and Harris et al. (2004a) to calculate the continuous opacity contributions from H I, H^-, He^-, He I, He II bound–free and free–free, H_2^- free–free, Rayleigh scattering of He I, H_2 and H I, Thomson scattering by e^- and H_2^+ free–free and bound–free. Finally, H I line absorption is included by using the STARK subroutine from the ATLAS12 program (Kurucz 1993). For more details concerning program LOMES, see Harris et al. (in preparation).

Harris et al. (2004a) showed that H_3^+ influences the opacity of metal-poor stars. H_3^+ contributes to opacity both through electron donation and by direct absorption. In fact, in a zero-metallicity gas there are four different mechanisms which control the opacity (Lenzuni, Chernoff & Salpeter 1991): collision-induced absorption by H_2; Rayleigh scattering by H, H_2 and He; Thomson scattering by e^- and free–free and bound–free absorption by H^-. The last mechanism dominates the opacity at densities which can be found in stellar atmospheres (10^{-10} g cm$^{-3} \leqslant \rho \leqslant 10^{-6}$ g cm^{-3}), at temperatures between 3500 and 7000 K and it was shown (Harris et al. 2004a) that H_3^+, acting as an electron donor, increased the abundance of H^- and hence the opacity. Furthermore, H_3^+ was found to contribute up to 15 per cent to the opacity via line absorption. This is far smaller than its indirect effect on the opacity through electron donation (it can increase the opacity by a factor of 3). On the other hand, the effect of H_3^+ on the opacity is only important at densities higher than 10^{-8} g cm^{-3}. So, for very low-metallicity stars having a very low density, the molecular ion HeH^+ could have an effect on their opacity because of its strong dipole moment, particularly in cases where the He to H ratio is high.

3.2.1 The number density of HeH$^+$ and its isotopologues

In this work we use the LOMES equation of state subroutine, which is an improved version of the equation of state used by Harris et al. (2004a). LOMES was developed for use in modelling of very low-metallicity stellar atmospheres. It takes account of what are likely to be the 12 most common elements in very low-metallicity stars: H, He, C, N, O, Ne, Na, Mg, Si, S, Ca and Fe. The cations and anions of these atoms are accounted for as are the molecular ions H_2^+, H_2^-, H_3^+ and HeH^+. Finally LOMES currently considers the molecules CO, CN, C_2, CH, OH, NH, NO, O_2, N_2, CS, HCN, H_2O and their cations and anions.

LOMES uses the Saha equation to build a set of 13 non-linear simultaneous conservation equations. These equations are then solved for molecular equilibrium by using a multivariable Newton–Raphson iteration. This technique has been well documented in the past (e.g. Kurucz 1970). The LOMES subroutine assumes a pre-set metal mix, and takes input of hydrogen, helium and metal number fraction, as well as temperature. The user can choose either density or pressure as the final state variable. LOMES returns the density or pressure along with the number densities of the 87 species including electrons.

In this work we focus on pure hydrogen–helium mixes, so that we set the metal number fraction to near zero (10^{-30}). This allows us to avoid the potential numerical problems of setting the number fraction to zero, while the effects of the metals are insignificant.

The number density $N_{\rm HeH}$ of HeH^+ was calculated by the program and we had to find the proportions of the different isotopologues in the number density of HeH^+. As we were interested in metal-poor stars formed from primordial material, we considered that the proportions of the isotopologues of HeH^+ were the same as in the primordial Universe.

To find these proportions, we used data given in Coc et al. (2004). They used both standard big bang nucleosynthesis (SBBN) and recent *WMAP* results to calculate the primordial ^{4}He mass fraction and the abundance ratio of D/H and ^{3}He/H. Both SBBN and *WMAP* are used to determine the baryonic density (density of ordinary matter) in the Universe. The SBBN is a method based on nuclear physics in the early Universe whereas *WMAP* studies the cosmic microwave background anisotropies to deduce the baryonic parameter $\Omega_{\rm b}h^2$ (where H is the Hubble constant expressed in units of 100 km s^{-1} Mpc^{-1}). The *WMAP*+SBBN results were $Y_p = 0.2479 \pm 0.0004$ for the ^{4}He mass fraction, $^3{\rm He/H} = (1.04 \pm 0.04) \times 10^{-5}$ and ${\rm D/H} = (2.60^{+0.19}_{-0.17}) \times 10^{-5}$.

Thus, we used number densities

$1.25 \times 10^{-4}\ N_{\rm HeH}$ for $^3HeH^+$,
$2.60 \times 10^{-5}\ N_{\rm HeH}$ for $^4HeD^+$,
$3.26 \times 10^{-9}\ N_{\rm HeH}$ for $^3HeD^+$, and
$[1 - (1.25 \times 10^{-4} + 2.60 \times 10^{-5} + 3.26 \times 10^{-9})]N_{\rm HeH}$ for $^4HeH^+$.

The total opacity was obtained by summing each opacity multiplied by the corresponding density fraction. We investigated the effect of HeH^+ on the opacity of zero-metallicity stars for different conditions; the results are discussed in the next section.

4 RESULTS AND DISCUSSION

In order to determine the importance of HeH^+ in zero-metallicity stars, we have calculated the total opacity for different temperatures T, densities ρ and hydrogen number fractions X_n. The total opacity takes account of all the hydrogen and helium species including H_3^+ but with or without HeH^+ to investigate its effect.

First we made a calculation using the solar hydrogen number fraction ($X_n = 0.92$) and a temperature of 3500 K where the effect of H_3^+ is maximum (Harris et al. 2004a). The effect of H_3^+ on the opacity is only important at high densities ($\rho \geqslant 10^{-8}$ g cm^{-3}).

As a result, for low-metallicity stars having very low density, we find very weak lines caused by the molecular ion HeH^+. HeH^+ contributes to opacity only for wavenumbers between 0 and 5000 cm^{-1} (see Fig. 1).

At temperatures higher than 4000 K neither HeH^+ lines nor H_3^+ lines are visible; this is because the opacity created by H^- increases

much faster with the temperature than the opacity created by HeH^+ and the effect of H_3^+ is only important for temperatures lower than 3500 K.

At lower temperatures, around 3000 K, H_3^+ lines dominate and no HeH^+ lines are visible.

Finally, for densities higher then 10^{-8} g cm^{-3} one can neglect HeH^+ lines if the number fraction of helium is solar. However, they become visible, but not very important, at densities lower than 10^{-10} g cm^{-3} and for a temperature around 3500 K.

We then decreased the hydrogen number fraction ($X_n = 0.8$–0.1), which means we increased the helium number fraction. We found that HeH^+ lines become more important as the helium number fraction increases.

Keeping the hydrogen number fraction equal to 0.1, we varied the temperature and the density. With this high helium number fraction, HeH^+ lines are clearly visible for higher densities from 10^{-8}, even 10^{-6} g cm^{-3}; their maximum effect is for a density of 10^{-9} g cm^{-3} and a temperature of 3500 K (see Fig. 2).

For a high helium number fraction, HeH^+ lines become important even for densities around 10^{-8} g cm^{-3} and are more important for a temperature around 3500 K. Thus the helium number fraction seems to be the most important parameter in determining the role of HeH^+. Thus, if one hopes to detect HeH^+ in the atmosphere of a star, the best conditions are a very low density ($\rho \leqslant 10^{-9}$ g cm^{-3}), a temperature around 3500 K and a high number fraction of helium.

As H_3^+, HeH^+ influences the opacity by direct absorption and by electron donation, but our tests showed the latter is unimportant compared to the direct absorption. Indeed, we checked the effect of HeH^+ as an electron donor. For a hydrogen number density of 0.1 or less, the effect of the electron donation by HeH^+ becomes important but only for high densities ($\rho \geqslant 10^{-4}$ g cm^{-3}).

5 CONCLUSION

We have calculated all the energy levels of $^4HeH^+$, $^3HeH^+$, $^4HeD^+$ and $^3HeD^+$ and the Einstein A coefficients corresponding to each rotation–vibration transition and pure rotational transitions. Thus we have obtained complete line lists for all the isotopologues of HeH^+. These transition data could also be important for nebular and interstellar studies. The partition functions of each isotopologue have been computed by direct summation of the energy levels. These data have been then used to calculate the opacity of HeH^+.

The total opacity has been calculated for zero-metallicity gas, taking account of the isotopic composition of the primordial Universe. We have used an updated version of the program which was used to investigate the effect of H_3^+ by Harris et al. (2004a). The total opacity has been calculated for different temperatures, densities and number fraction of hydrogen.

We have checked the validity of the effective neglect of the molecular ion HeH^+ adopted by Harris et al. (2004a) when they studied the effect of H_3^+. Their results are correct because they were interested in high densities, around 10^{-6} g cm^{-3} and in a solar helium number fraction. However, HeH^+ lines become visible for very low densities (10^{-10} g cm^{-3}) when the helium number fraction is solar, and for temperatures near 3500 K. Moreover, when the helium number fraction is high (0.9), HeH^+ lines can be strongly seen for higher densities ($\rho \leqslant 10^{-6}$ g cm^{-3}) and are still more important for a temperature around 3500 K and a density of 10^{-9} g cm^{-3}.

The stars whose observed energy distributions were analysed by Bergeron & Leggett (2002) seem to satisfy these conditions. Indeed, Bergeron & Leggett (2002) studied two cool white dwarfs, LHS 3250 and SDSS 1337 + 00, and showed that the best predictions for their observed energy distributions were given by simulations using extreme helium compositions. They concluded that their cool white dwarfs should have helium-rich atmospheres and effective temperatures below 4000 K. The simulations closest to their observations for these stars were for low masses (less than 0.7 $M_\odot$), temperatures around 3300 K and very high He to H ratios (more than 10^3). These stars seem to be good candidates to look for HeH^+. HeH^+ appears to have been largely neglected in atmospheric models for cool white dwarfs (Stancil 1994; Bergeron et al. 2001). A study of the effects of including HeH^+ in cool helium-rich white dwarfs will be presented elsewhere (Harris et al. 2004b).

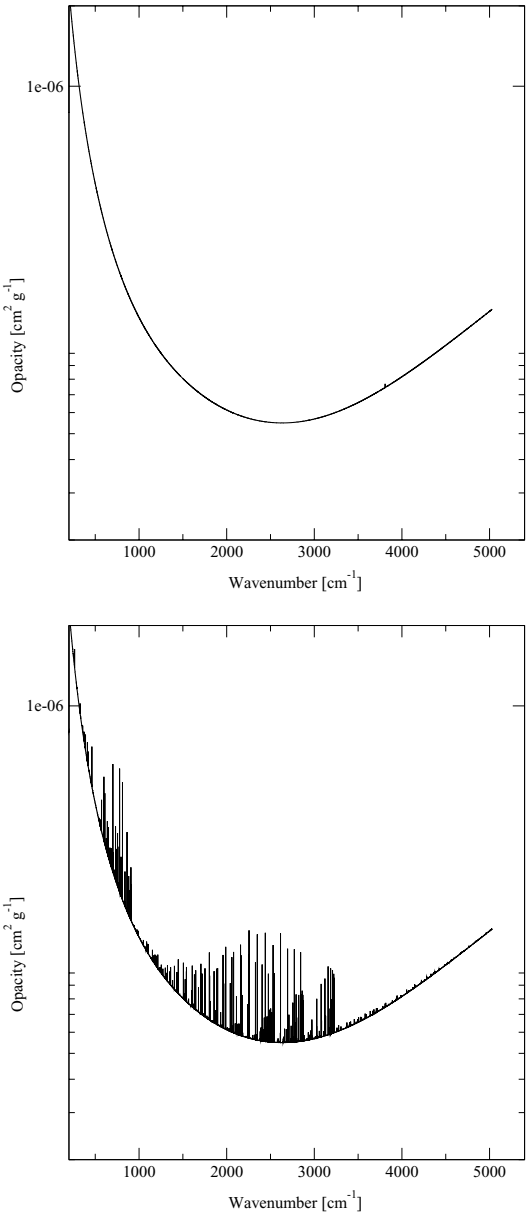

Figure 2. Opacity function taking account of all the hydrogen and helium species, including H_3^+ in the upper graph and including H_3^+ and HeH^+ in the lower graph, for a density $\rho = 10^{-9}$ g cm^{-3}, a temperature $T = 3500$ K and a hydrogen number fraction $X_n = 0.1$.

ACKNOWLEDGMENTS

We thank Tony Lynas-Gray for helpful discussions, the UK Particle Physics and Astronomy Research Council (PPARC) and the

Engineering and Physical Sciences Research Council (EPSRC) for funding. EAE is also grateful to the Région Rhône Alpes for supporting her visit to University College London.

REFERENCES

Bergeron P., Leggett S. K., 2002, ApJ, 580, 1070
Bergeron P., Leggett S. K., Ruiz M. T., 2001, ApJS, 133, 413
Bishop D. M., Cheung L. M., 1979, J. Molec. Spect., 75, 462
Cecchi-Pestellini C., Dalgarno A., 1993, ApJ, 413, 611
Christlieb N. et al., 2002, Nat, 419, 904
Coc A., Viangioni-Flam E., Descouvemont P., Adahchour A., Angulo C., 2004, ApJ, 600, 544
Coxon J. A., Hajigeorgiou P. G., 1999, J. Molec. Spect., 193, 306
Faure A., Tennyson J., 2001, MNRAS, 325, 443
Green T. A., Browne J. C., Michels H. H., Madsen M. M., 1974, J. Chem. Phys., 61, 12
Harris G. J., Lynas-Gray A. E., Miller S., Tennyson J., 2004a, ApJ, 600, 1025
Harris G. J., Lynas-Gray A. E., Miller S., Tennyson J. 2004b, ApJ, 617, L43
Irwin A. W., 1981, ApJS, 45, 621
Kashlinsky A., Rees M. J., 1983, MNRAS, 205, 995
Kolos W., Peek J. M., 1976, Inter. J. Quant. Chem., Vol. X, 217
Kurucz R. L., 1970, Smithsonian Obs. Spec. Rep., p. 308
Kurucz R. L., 1993, in Dworetsky M. M., Castelli F., Faraggiana R., eds, ASP Conf. Ser. Vol. 44, IAU Coll. 138, Peculiar Versus Normal Phenomena in A-Type and Related Stars. Astron. Soc. Pac., San Fransisco, p. 87
Kurucz R. L., 2000, http://kurucz.harvard.edu/linelists.html
Lenzuni P., Chernoff F. P., Salpeter E. E., 1991, ApJ, 76, 759
Lepp S., Stancil P. C., Dalgarno A., 2002, J. Phys. B, 35, R57
Le Roy R. J., 2002, LEVEL 7.5, Univ. Waterloo Chemical Physics Research Report CP-655, http://scienide.uwaterloo.ca/∼leroy/level/
Liu X.-W. et al., 1997, MNRAS, 290, L71
Miller S., Tennyson J., Lepp S., Dalgarno A., 1992, Nat, 355, 420
Moorhead J. M., Lowe R. P., Maillard J.-P., Wehlau W. H., Bernath P. F., 1988, ApJ, 326, 899
Morel P., 1997, A&A, 124, 597
Morel P., Baglin A., 1999, A&A, 345, 156
Rabadan I., Sarpal B. K., Tennyson J., 1998, MNRAS, 299, 171
Saenz A., 2003, Phys. Rev. A, 67, 033409
Saio H., Jeffery C. S., 2000, MNRAS, 313, 671
Sauval A. J., Tatum J. B., 1984, ApJS, 56. 193
Stancil P. C., 1994, ApJ, 430, 360
Zygelman B., Stancil P. C., Dalgarno A., 1998, ApJ, 508, 151

This paper has been typeset from a TEX/LATEX file prepared by the author.